14th Australasian Fluid Mechanics Conference
Adelaide University, Adelaide, Australia
9-14 December 2001

Numerical Study on the Dynamics of a Cavitation Bubble near a Rigid Body

M.T. Shervani-Tabar[1] and Kh. Arshadi[2]

[1] Department of Mechanical Engineering
University of Tabriz, Tabriz, Iran
[2] Tabriz Petrochemical Company
Tabriz, Iran

Abstract

Cavitation damage in structures is of universal interest and concern. Cavitation bubbles are produced in liquid flows when the liquid pressure drops below the saturated vapour pressure. These bubbles flow with liquid and collapse in the high pressure region. The collapse of a cavitation bubble in the vicinty of a rigid boundary is accompanied by a high velocity liquid jet. The liquid jet, in the absence of buoyancy forces, forms on the side of the bubble far from the rigid boundary and is directed towards it. The impingment of the liquid jet to the rigid boundary is believed to be one of the important factors of cavitation damage. In this paper dynamics of a cavitation bubble near a rigid body is studied using the Boundary Element Method.

Numerical study of growth and collapse of a cavitation bubble near a rigid body gives detailed information about the migration of the bubble away or towards the rigid body, the volume change of the bubble during its growth and collapse and the formation of the liquid jet. Development and direction of the liquid jet is studied in different cases.

Introduction

Cavitation is favored anywhere low-pressure regions form in water. Bubbles are formed when the liquid pressure drops its vapour pressure. Experimental investigations [1,4,5,6] show that when a bubble subsequently collapse near a rigid surface, a liquid jet is developed on the side of the bubble far from the rigid surface and directed towards it. The impingment of the liquid jet on the rigid surface causes local stress that can be great enough to cause plastic deformation of many metals. Cavitation commonly occurs on ship propellers, centrifugal pump and turbine blades and other surfaces that encounters high local liquid velocities and large liquid static pressure gradients.

A computer simulation of a cavitation vapour bubble is carried out using the boundary integral equation technique to show the growth and collapse of the bubble above and below a rigid body. Computer study of the cavitation bubbles is of great importance in medicine because of their role in the disintegration of kidney stones and gallstones by Extracorporeal Shock Wave Lithotripsy [6,8].

Geometrical Definition

As illustrated in Figure 1 the vapour bubble is located in the liquid domain in the vicinity of a spherical rigid body. The polar cylindrical axes are chosen with the vertical axis piercing the centre of the spherical rigid body and the centroid of the bubble. The radial axis pierces the centre of the rigid body.

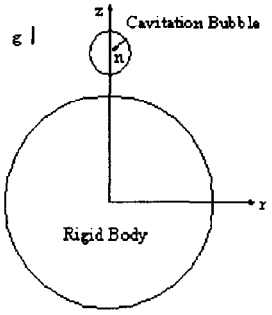

Figure 1 Geometrical definition for a bubble collapsing near a spherical rigid body

Hydrodynamic Equation

The fluid flow is assumed to be incompressible, inviscid and irrotational and the surface tension on the bubble boundary is neglected. Thus the fluid flow behaves in the framework of potential flow and the velocity in the liquid domain and on the bubble boundary can be represented as the gradient of a potential which satisfies Laplace's equation. In this case the Green's formula may be written as

$$c(p)\phi(p) + \int_{S_b+S_r} \phi(q)\frac{\partial}{\partial n}\left(\frac{1}{|p-q|}\right)ds = \int_{S_b+S_r} \frac{\partial}{\partial n}\left(\phi(q)\right)\frac{1}{|p-q|}ds \qquad (1)$$

where $\phi(p)$ is the velocity potential, S_b is the surface of the bubble, S_r is the surface of the rigid body, p is any given point in the liquid domain or on S, which includes S_b and S_r and q is a point on S. Therefore $c(p)$ is 4π when p belongs to the liquid domain and is 2π if p is on S.

The unsteady Bernoulli's equation, in Lagrangian form, is given by:

$$\frac{D\phi}{Dt} = \frac{P_\infty - P_c}{\rho} + \frac{1}{2}|\nabla\phi|^2 + g(z-h) \qquad (2)$$

where P_∞ is the ambient pressure, P_c is the vapour pressure in the bubble, ρ is the density of the liquid and h is the distance between the bubble and the rigid body and z is the vertical distance of any point from the horizontal axis.

Discretized Approximation

The surface of the bubble is discretized into N segments. To overcome the non-smooth nature of the piecewise linear interpolation, cubic splines are employed to approximate the surface of the bubble. Velocity potentials over the bubble surface are assumed to be constant over each element and are located at the midpoint of elements. The surface of the rigid body is discretized into M segments. Let s_j represents the j_{th} segment. Then for a point p_i on the surface of the bubble and on the surface of the rigid body, the discretized form of equation (1) is given by

$$2\pi\phi(p_i)+\sum_{j=1}^{N+M}\left\{\phi(q_j)\int_{s_j}\frac{\partial}{\partial n}\left[\frac{1}{p_i+q_j}\right]ds\right\} = \sum_{j=1}^{N+M}\left\{\frac{\partial}{\partial n}\left[\phi(q_j)\right]\int_{s_j}\left[\frac{1}{p_i+q_j}\right]ds\right\} \quad (3)$$

The surface integrations are carried out analytically where p, chosen as a collocation point, is located at the middle of the i_{th} segment. The term $\frac{\partial\phi}{\partial n}$ is the velocity component normal to the surface of the bubble and is denoted by ψ. It should be noted that ψ is positive when it is directed into the bubble. Thus equation (3) becomes a system of linear equations in the form of

$$2\pi\phi(p_i)+\sum_{j=1}^{N+M}H_{ij}\phi(q_j)=\sum_{j=1}^{N+M}G_{ij}\psi(q_j) \quad (4)$$

where H_{ij} and G_{ij} are the terms of integration in equation (3) which are integrated over each segment. From equation (3) the normal velocity on the bubble surface and the velocity potential on the surface of the rigid body are calculated. The tangential velocity, η, can be obtained for every given distribution of velocity potential ϕ.

The implementation of the second order Runge-Kutta integration is as follows. At time t the collocation point is represented by a vector p_i with cylindrical polar coordinates of r_i and z_i. The velocity potential at time t is represented by ϕ_i. Then by solving equation (4) the fluid velocity at the collocation points, ψ_i, are determined. By having ψ_i and η_i the radial and vertical components of the fluid velocity (u_i, v_i) can be obtained. Then it can be written

$$r_{i1}=r_i(t)+u_{i1}\Delta t, \quad (5)$$

$$z_{i1}=z_i(t)+v_{i1}\Delta t, \quad (6)$$

$$\phi_{i1}=\phi_i(t)+\left[\frac{\partial\phi}{\partial t}\right]_{i1}\Delta t. \quad (7)$$

Equation (4) is solved for the intermediate geometry of the bubble and the intermediate distribution of the velocity potential over the bubble surface and the surface of the rigid body. Then the intermediate velocity on the bubble surface (u_{i2}, v_{i2}) and the intermediate derivative of the velocity potential $\left[\frac{\partial\phi}{\partial t}\right]_{i2}$ are obtained. The evolved shape of the bubble and the distribution of the velocity potential over its surface at time $t+\Delta t$ are given by

$$r_i(t+\Delta t)=r_i(t)+\frac{1}{2}(u_{i1}+u_{i2})\Delta t+0(\Delta t^2), \quad (8)$$

$$z_i(t+\Delta t)=z_i(t)+\frac{1}{2}(v_{i1}+v_{i2})\Delta t+0(\Delta t^2) \quad (9)$$

$$\phi_i(t+\Delta t)=\phi_i(t)+\frac{1}{2}\left(\left[\frac{\partial\phi}{\partial t}\right]_{i1}+\left[\frac{\partial\phi}{\partial t}\right]_{i2}\right)\Delta t+0(\Delta t^2). \quad (10)$$

It should be noted that the velocity vector (u_i, v_i), along the direction of r and z are derived from the velocity components that are normal to the bubble surface, ψ_i, and tangential to it, η_i.

Numerical Results and Discussion

Figure 2 illustrates the growth and collapse of a cavitation bubble from its initially spherical shape at minimum volume and in the absence of buoyancy forces. The bubble is located above the rigid body. It is shown that in the absence of buoyancy forces the cavitation bubble during its collapse phase migrates towards the rigid body and a liquid jet is developed on the side of the bubble far from the rigid body and directed towards it.

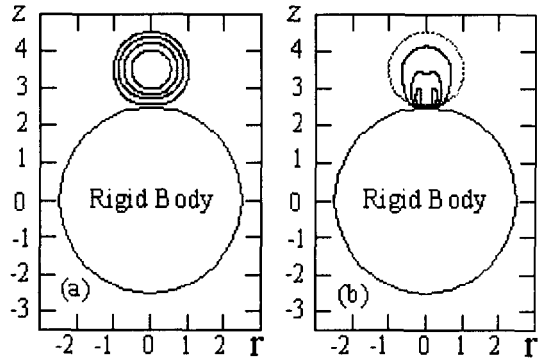

Figure 2 Bubble shapes for the growth (a) and collapse (b) of a cavitation bubble above a rigid body with $\gamma = 1.0$ and in the absence of buoyancy forces. The non-dimensional time to bubble successive profiles are: (a) Growth phase: 0.0187 (innermost), 0.1493, 0.3314, 1.0787 (outermost). (b) Collapse phase: 1.0787 (outermost), 1.6745, 1.8668, 1.9283 (innermost).

Non-dimensional Time= $\frac{t}{R_{\max}}\left(\frac{P_\infty - P_c}{\rho}\right)^{\frac{1}{2}}$, $\gamma = \frac{h}{R_{\max}}$

Figure 3 illustrates the growth and collapse of a buoyant cavitation bubble above a rigid body. This figure shows that in the case of strong buoyancy forces the bubble migrates away from the rigid body.

In this case during the collapse phase of the bubble an annular liquid jet is developed at the lower part of the bubble and splits the bubble into two parts. This type of phenomenon has been observed by Gibson and Blake [2] near flexible boundaries, and by Taib [3] for the growth and collapse of a buoyant vapour bubble in an axisymmetric stagnation point flow near a rigid boundary.

Figure 4 illustrates the growth and collapse of a cavitation bubble below a rigid body considering buoyancy forces. This figure shows that in contrast with the case of the buoyant bubble above the rigid body, strong buoyancy forces in the direction of Bjerknes attraction force through the rigid body can cause the

development of a strong liquid jet directed towards the rigid body.

The change in volume of the bubble in different cases is shown in Figure 5. This figure indicates that below a rigid body the collapse rate of a buoyant bubble is higher than the collapse rate of a bubble without buoyancy forces. It can also be seen that above the rigid body the collapse rate of a bubble without buoyancy forces is higher than the collapse rate of a buoyant bubble.

Figure 6 illustrates the effect of the buoyancy forces on the migration of the bubble either towards the rigid body or away from it. Figure 6 indicates that in the case of a bubble above the rigid body, strong buoyancy forces cause the migration of the bubble away from the rigid body.

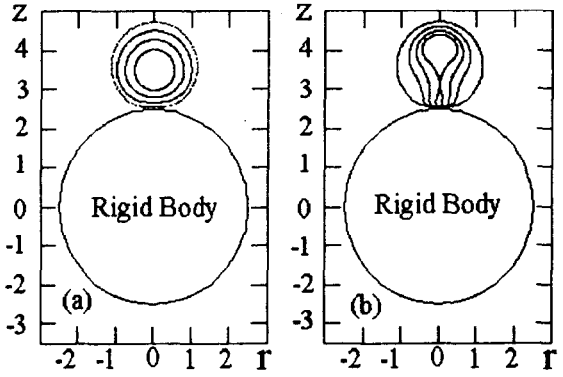

Figure 3 Bubble shapes for the growth (a) and collapse (b) of a buoyant cavitation bubble above a rigid body with $\gamma = 1.0$ and $\delta = 0.3132$. The non-dimensional time to bubble successive profiles are: (a) Growth phase: 0.0141 (innermost), 0.1854, 0.4844, 1.2630 (outermost). (b) Collapse phase: 1.2630 (outermost), 2.0939, 2.2865, 2.3928 (innermost).

$$\delta = \left(\frac{\rho g R_{max}}{P_\infty - P_c} \right)^{\frac{1}{2}}$$

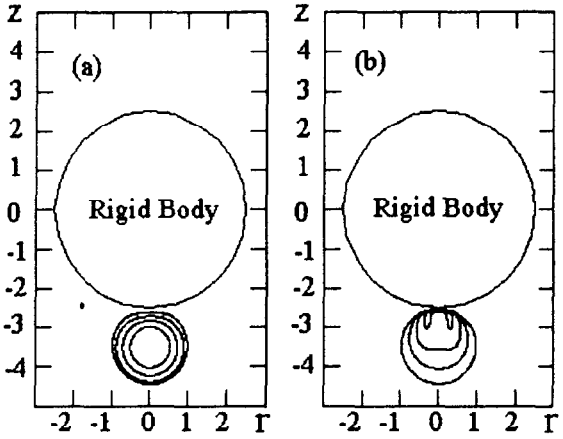

Figure 4 Bubble shapes for the growth (a) and collapse (b) of a buoyant cavitation bubble below a rigid body with $\gamma = -1.0$ and $\delta = 0.3132$. The non-dimensional time to bubble successive profiles are: (a) Growth phase: 0.0124 (innermost), 0.1232, 0.3233, 0.7815 (outermost). (b) Collapse phase: 0.7815 (outermost), 1.2808, 1.4779, 1.6095 (innermost).

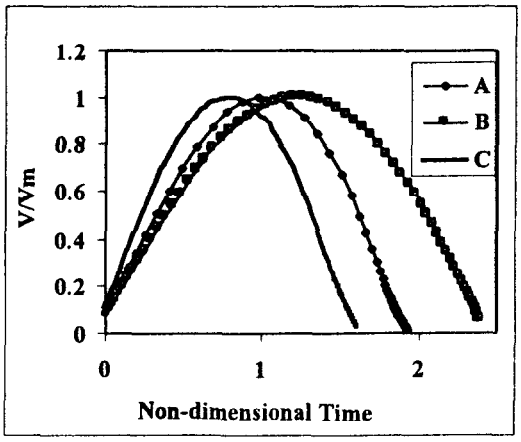

Figure 5 Variation of the bubble volume during its growth and collapse phases in the cases of: (A) a cavitation bubble above a rigid body with $\gamma = 1.0$ and in the absence of buoyancy forces, (B) a buoyant cavitation bubble above a rigid body with $\gamma = 1.0$ and $\delta = 0.3132$ and (C) a buoyant cavitation bubble below a rigid body with $\gamma = -1.0$ and $\delta = 0.3132$.

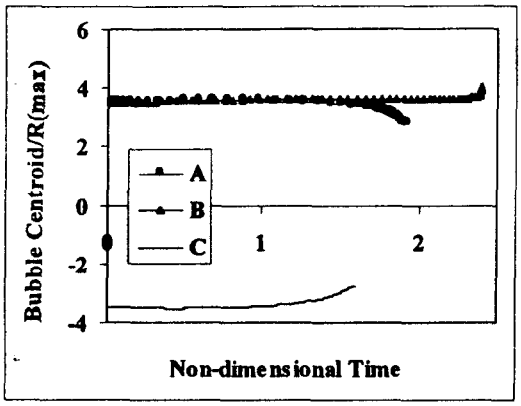

Figure 6 Migration of the bubble centroid during its growth and collapse phases in the cases of: (A) a cavitation bubble above a rigid body with $\gamma = 1.0$ and in the absence of buoyancy forces, (B) a buoyant cavitation bubble above a rigid body with $\gamma = 1.0$ and $\delta = 0.3132$ and (C) a buoyant cavitation bubble below a rigid body with $\gamma = -1.0$ and $\delta = 0.3132$.

Conclusions

In this paper dynamics of a collapsing cavitation bubble in the vicinity of a rigid body has been investigated using a computer model based on the boundary integral equation method.

Results show that in the absence of buoyancy forces a high speed liquid jet is developed on the side of the bubble far from the rigid body and directed towards it. Results also show that the development of the high speed liquid jet towards the rigid body occurs in a very short period of time.

It has been shown that buoyancy forces have sigificant effect on the dynamics of the bubble. Strong buoyancy forces acting opposite to the Bjerknes attraction force through the rigid body may cause the develpment of a liquid jet on the side of the bubble close to the rigid body and directed away from it.

Acknowledgements

The authors acknowledge the support of the University of Tabriz.

References

[1] Best, J.P., Soh, W.K. and Yu, C.F. (1996), " An experimantal investigation of buoyant transient cavity collapse near rigid cylindrical boundaries", J. Fluid Eng., Vol. 118, pp. 195-198.

[2] Gibson, D.C. and Blake,J.R. (1982), " The growth and collapse of bubbles near deformable surfaces", Applied Scientific Research, 38, pp. 215-224.

[3] Taib, B.B. (1985), " Boundary integral method applied to cavitation bubble dynamics", Ph.D. Thesis, University of Wollongong, Australia.

[4] Tomita, Y. and Shima, A. (1986), " Mechanisms of impulsive pressure generation and damage pit formation by bubble collapse", J. Fluid Mech., Vol. 169, pp. 535-564.

[5] Tomita, Y. and Shima, A. (1990), " High-speed observations of laser-induced cavitation bubbles in water", Acoustica, Vol. 71, pp. 161-171.

[6] Vakil, N., Grasewski, S.M. and Everbach, C.E. (1991), " Relationship to model stone properties to fragmentation mechanisms during lithotripsy", Journal of lithotripsy and stone disease, Vol. 3, No. 4, pp. 304-310.

[7] Wong, K.C., Soh, W.K. and Blake, J.R. (1989), " High speed flow visualization of a cavitation bubble", Proceedings of the Tenth Australasian Fluid Mechanics Conference, The Institution of Engineers, Australia, Melbourne, December, pp. 227-230.

[8] Zhong, P. and Choung, C.J. (1993), " Propagation of shock waves in elastic solids caused by cavitation micro jet impact. II: Application in extracorporeal shock wave lithotripsy", J. Acoust. Soc. Am. 94 (1), pp. 29-36, July.